

Supplementary Materials

Amorphous RuCoP ultrafine nanoparticles supported on carbon as efficient catalysts for hydrogenation of adipic acid to 1,6-hexanediol

Wei Gong ¹, Xuyun Wang ^{1,*}, Shan Ji ² and Hui Wang ^{1,*}

¹ State Key Laboratory Base for Eco-Chemical Engineering, College of Chemical Engineering, Qingdao University of Science and Technology, Qingdao 266042, China

² College of Biological, Chemical Science and Chemical Engineering, Jiaying University, Jiaying 314001, China

* Correspondence: wangxy@qust.edu.cn (X.W.); wangh@qust.edu.cn (H.W.)

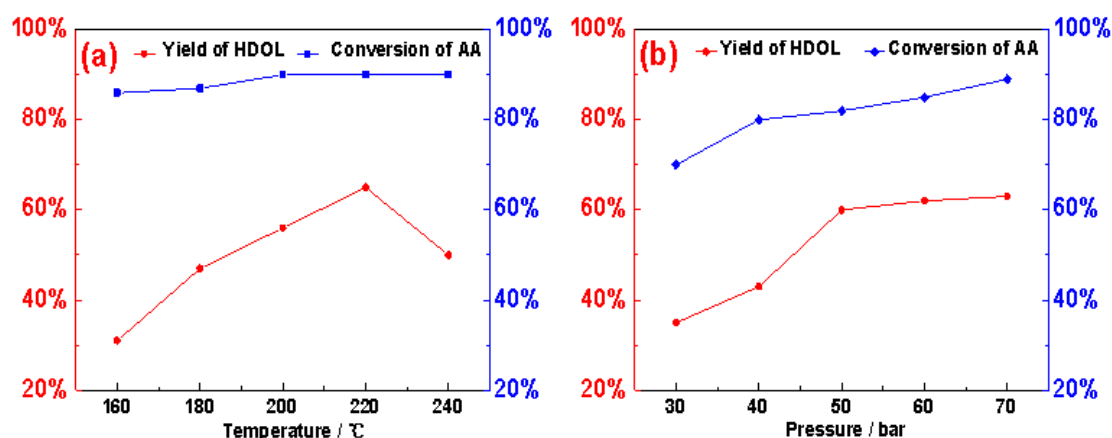
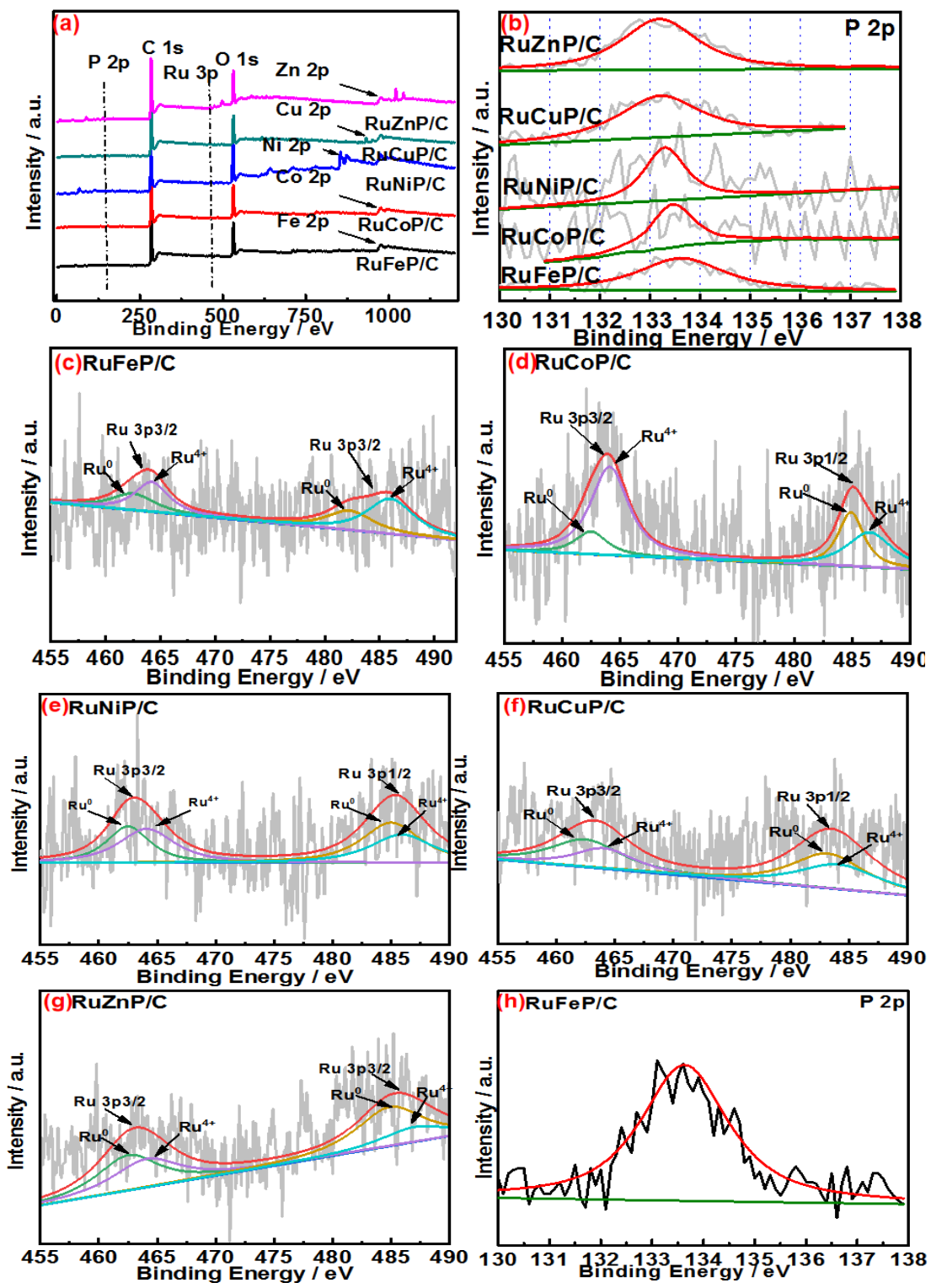


Figure S1. Effect of temperature (a) and pressure (b) on AA conversion and HDOL selectivity.



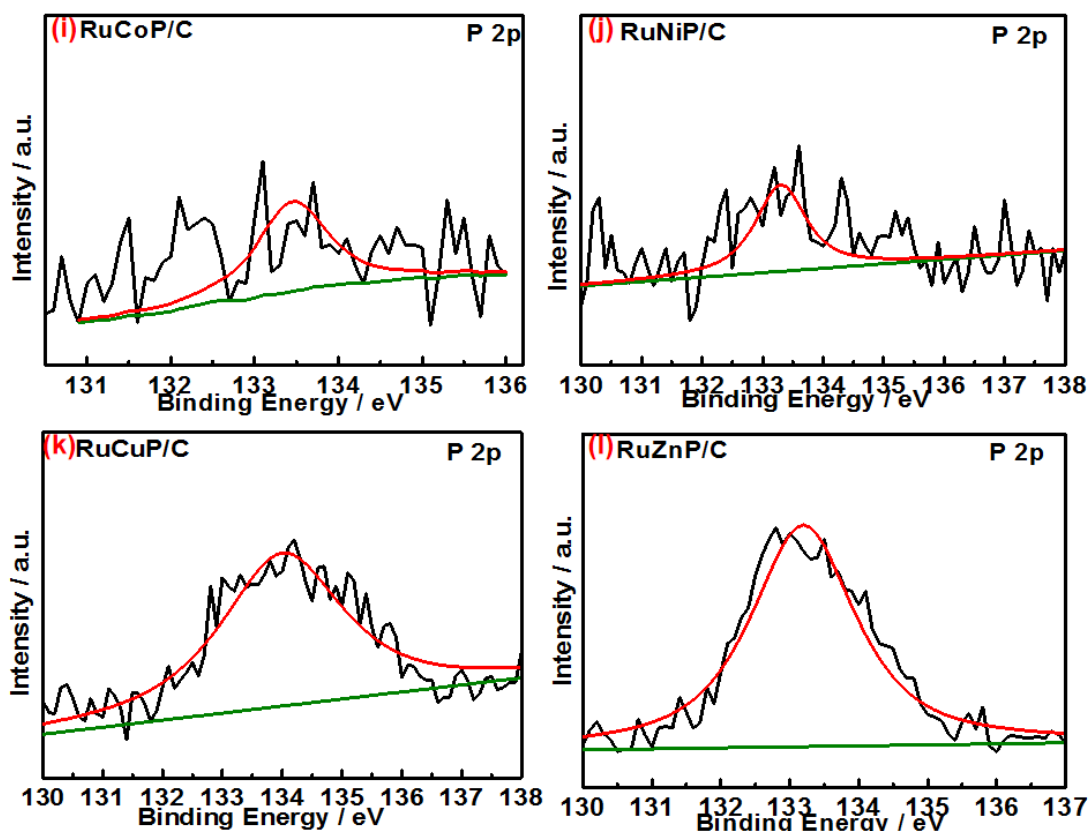


Figure S2. XPS survey spectra of all the alloys (a); P 2p XPS spectra of the different metal-doped alloy(b); Ru 3p XPS spectra of RuFeP(c), RuCoP(d) , RuNiP (e), RuCuP(f) and RuZnP(g) and P 2p XPS spectra of RuFeP(h) , RuCoP(i), RuNiP (j), RuCuP (k) and RuZnP (l).

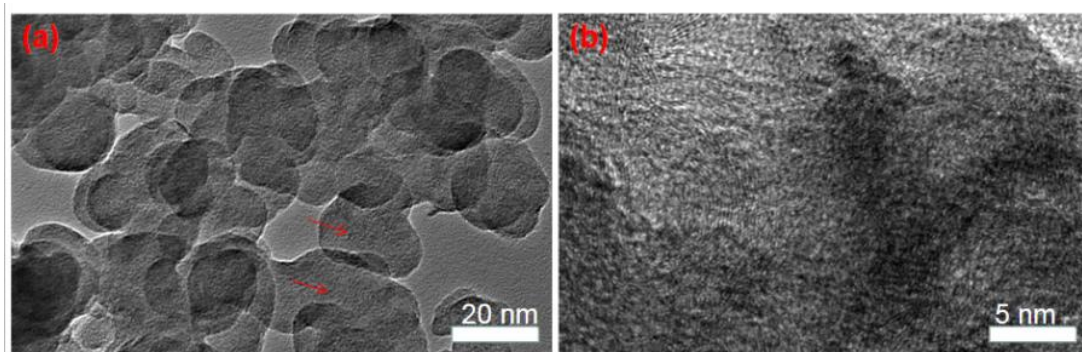


Figure S3. TEM images (a and b) of RuCoP/C.

Table S1. Assignments binding energies (BEs) and concentrations of Ru 3p species in as-prepared alloys from Ru 3p XPS spectra.

Catalyst	Ru 3p	BE ^a	Concentration ^b
RuFeP/C	Ru ⁰	462.5, 482.5	0.42
	Ru ⁴⁺	464.5, 486	0.58
RuCoP/C	Ru ⁰	462.5, 485	0.53
	Ru ⁴⁺	464, 486.5	0.47
RuNiP/C	Ru ⁰	462.5, 485	0.49
	Ru ⁴⁺	464, 486	0.51
RuCuP/C	Ru ⁰	462.5, 483	0.63
	Ru ⁴⁺	464, 484	0.37
RuZnP/C	Ru ⁰	462.5, 485	0.45
	Ru ⁴⁺	464.5, 487.5	0.55

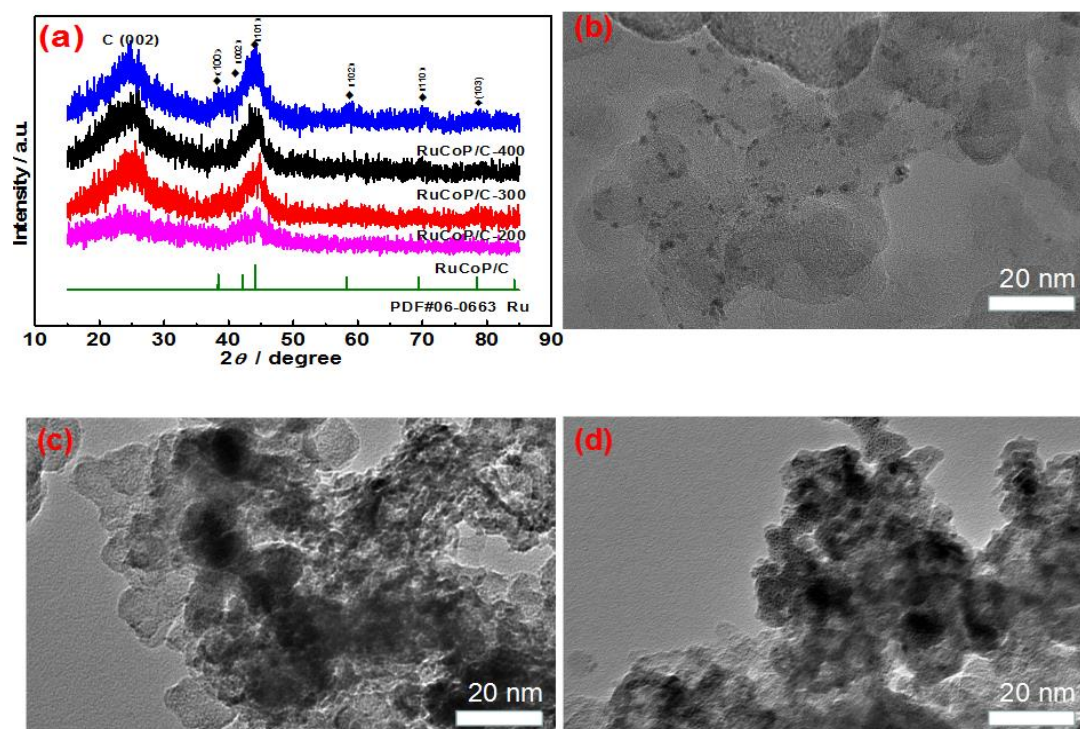


Figure S4. (a) XRD patterns of RuCoP samples heat-treated at different temperatures. TEM images of RuCoP/C-200(b), RuCoP/C-300 (c) and RuCoP/C-400 (d).

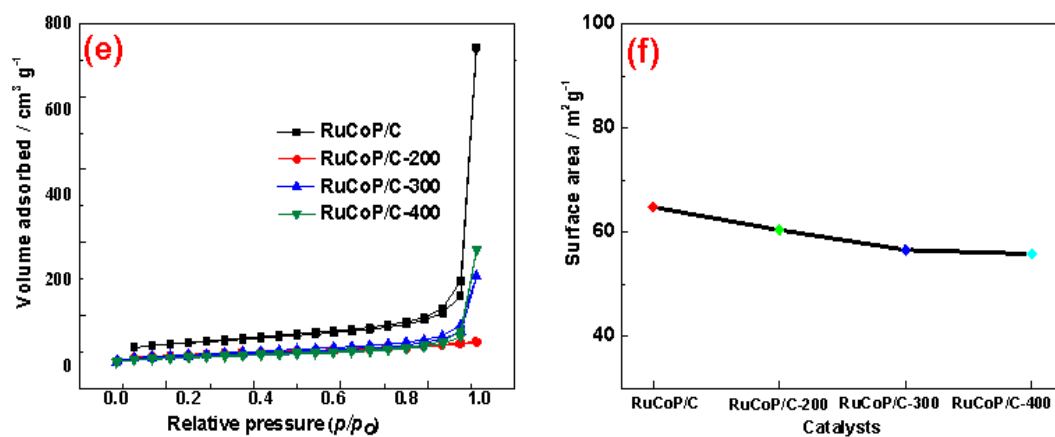


Figure S5. N₂ adsorption and desorption isotherm (e), and BET surface areas of RuCoP/C treated at various temperatures (f).